A general theory of discrete filtering for LES in complex geometry

By Oleg V. Vasilyev AND Thomas S. Lund

1. Motivation and objectives

In large eddy simulation (LES) of turbulent flows, the dynamics of the large scale structures are computed while the effect of the small scale turbulence is modeled using a subgrid scale model. The differential equations describing the space-time evolution of the large scale structures are obtained from the Navier-Stokes equations by applying a low-pass filter. In order for the resulting LES equations to have the same structure as the Navier-Stokes equations, the differentiation and filtering operations must commute. In inhomogeneous turbulent flows, the minimum size of eddies that need to be resolved is different in different regions of the flow. Thus the filtering operation should be performed with a variable filter width. In general, filtering and differentiation do not commute when the filter width is non-uniform in space.

The problem of non-commutation of differentiation and filtering with non-uniform filter widths was studied by Ghosal and Moin (1995), who proposed a new class of filters for which the commutation error could be obtained in closed form. The application of this filter to the Navier-Stokes equations introduces additional terms (due to commutation error) which are of second order in the filter width. Ghosal and Moin suggested that the leading correction term be retained if high order numerical schemes are used to discretize the LES equations. This procedure involves additional numerical complexities which can be avoided by using the filters described in this report. Van der Ven (1995) constructed a family of filters which commute with differentiation up to any given order in the filter width; however, this approach is limited to a specific choice of filters and does not address the issue of additional boundary terms that would arise in finite domains.

Due to the lack of a straightforward and robust filtering procedure for inhomogeneous flows, most large eddy simulations performed to date have not made use of explicit filters. The nearly universal approach for LES in complex geometries is to argue that the finite support of the computational mesh together with the low-pass characteristics of the discrete differencing operators effectively act as a filter. This procedure will be referred to as implicit filtering since an explicit filtering operation never appears in the solution procedure. Although the technique of implicit filtering has been used extensively in the past, there are several compelling reasons to adopt a more systematic approach. Foremost of these is the issue of consistency. While it is true that discrete derivative operators have a low-pass filtering effect, *the associated filter acts only in the one spatial direction in which the derivative is taken.* This fact implies that each term in the Navier-Stokes equations is acted on by a distinct one-dimensional filter, and thus there is no way to derive the discrete equations through the application of a single three-dimensional filter. Considering this ambiguity in the definition of the filter, it is nearly impossible to make detailed comparisons of LES results with filtered experimental data. In the same vein it is not possible to calculate the Leonard term (Leonard, 1974) that appears as a computable portion in the decomposition of the subgrid-scale stress.

The second significant limitation of the implicit filtering approach is the inability to control numerical error. Without an explicit filter, there is no direct control in the energy in the high frequency portion of the spectrum. Significant energy in this portion of the spectrum coupled with the non-linearities in the Navier-Stokes equations can produce significant aliasing error. Furthermore, all discrete derivative operators become rather inaccurate for high frequency solution components, and this error interferes with the dynamics of the small scale eddies. This error can be particularly harmful (Lund and Kaltenbach, 1995) when the dynamic model (Germano *et al.*, 1991; Ghosal *et al.*, 1995) is used since it relies entirely on information contained in the smallest resolved scales. In addition, it is difficult to define the test to primary filter ratio which is needed as an input to the dynamic procedure.

The difficulties associated with the implicit filtering approach can be alleviated by performing an explicit filtering operation as a part of the solution process. By damping the energy in the high frequency portion of the spectrum, it is possible to reduce or eliminate the various sources of numerical error that dominate this frequency range. Explicit filtering reduces the effective resolution of the simulation but allows the filter size to be chosen independently of the mesh spacing. Furthermore, the various sources of numerical error that would otherwise enter the stresses sampled in the dynamic model can be controlled, which can ultimately result in more accurate estimate for the subgrid scale model coefficient. Finally, the shape of the filter is known exactly, which facilitates comparison with experimental data and the ability to compute the Leonard term.

To realize the benefits of an explicit filter, it is necessary to develop robust and straightforward discrete filtering operators that commute with numerical differentiation. As mentioned above, the earlier works in this area required either adding corrective terms to the filtered Navier-Stokes equations or required the use of a restricted class of filters that could not account properly for non-periodic boundaries. The objective of this work is to develop a general theory of discrete filtering in arbitrary complex geometry and to supply a set of rules for constructing discrete filters that commute with differentiation to the desired order.

This report summarizes the essential results; the details of mathematical derivations and proofs are described by Vasilyev *et al.* (1997), hereafter denoted by VLM.

2. Accomplishments

2.1 Commutation error of filtering and differentiation operations

Consider a one-dimensional field $\psi(x)$ defined in a finite or infinite domain $[a, b]$. Let $f(x)$ be a monotonic differentiable function which defines the mapping from the domain $[a, b]$ into the domain $[\alpha, \beta]$, *i.e.* $\xi = f(x)$. $f(x)$ can be associated with mapping of the non-uniform computational grid in the domain $[a, b]$ to a uniform grid of spacing Δ, where the non-uniform grid spacing is given by $h(x) = \Delta / f^{'}(x)$.

Let $x = F(\xi)$ be the inverse mapping $(F(f(x)) = x)$. The filtering operation is defined in an analogous way as in (Ghosal and Moin, 1995). Given an arbitrary function $\psi(x)$, we obtain the new function $\phi(\xi) = \psi(F(\xi))$ defined on the interval $[\alpha, \beta]$. The function $\phi(\xi)$ is then filtered using the following definition:

$$\overline{\phi}(\xi) = \frac{1}{\Delta} \int_{\alpha}^{\beta} G\left(\frac{\xi - \eta}{\Delta}, \xi\right) \phi(\eta) d\eta, \tag{1}$$

where G is a filter function, which can have different shapes in various regions of the domain. This definition is more general then the one commonly used in the LES literature and, as will be shown later, is crucial for elimination of boundary terms in the commutation error. The introduction of filters of different shapes in different parts of the domain is necessitated by considering inhomogeneous (non-periodic) fields. If we assume that the function $\phi(\xi)$ is homogeneous (periodic) in $[\alpha, \beta]$, then a periodic filter can have the same shape throughout the domain.

The filtering operation in physical space can be written as

$$\overline{\psi}(x) = \frac{1}{\Delta} \int_{a}^{b} G\left(\frac{f(x) - f(y)}{\Delta}, f(x)\right) \psi(y) f^{'}(y) dy. \tag{2}$$

Note that definitions (1) and (2) are equivalent. However, the filtering operation (1) in the mapped space is much easier to analyze and implement than (2), and we will use it throughout unless stated otherwise.

Let us consider first the commutation error of filtering and derivative operations in one spatial dimension. We define an operator that measures commutation error by

$$\left[\frac{d\psi}{dx}\right] \equiv \overline{\frac{d\psi}{dx}} - \frac{d\overline{\psi}}{dx}. \tag{3}$$

Introducing the change of variables $\eta = \xi - \Delta\zeta$, Eq. (1) can be rewritten as

$$\overline{\phi}(\xi) = \int_{\frac{\xi-\beta}{\Delta}}^{\frac{\xi-\alpha}{\Delta}} G(\zeta, \xi) \phi(\xi - \Delta\zeta) d\zeta. \tag{4}$$

Performing the formal Taylor series expansion of $\phi(\xi - \Delta\zeta)$ in powers of Δ and changing the order of summation and integration, we obtain

$$\overline{\phi}(\xi) = \sum_{k=0}^{+\infty} \frac{(-1)^k}{k!} \Delta^k M^k(\xi) D_{\xi}^k \phi(\xi), \tag{5}$$

where $D_{\xi}^k \equiv \frac{d^k}{d\xi^k}$ is the derivative operator and $M^k(\xi)$ is the k-th filter moment defined by

$$M^k(\xi) = \int_{\frac{\xi-\beta}{\Delta}}^{\frac{\xi-\alpha}{\Delta}} \zeta^k G(\zeta, \xi) d\zeta. \tag{6}$$

The series (5) may have either infinite or finite radius of convergence depending on the filter moments. For the discrete filters, as shown in VLM, the radius of convergence of the series is infinity.

Substituting (5) into (3) and skipping the algebra we obtain

$$\left[\frac{d\psi}{dx}\right] = \sum_{k=1}^{+\infty} A_k M^k(\xi)\Delta^k + \sum_{k=0}^{+\infty} B_k \frac{dM^k}{d\xi}(\xi)\Delta^k, \tag{7}$$

where A_k ($k \geq 1$) and B_k ($k \geq 0$) are, in general, nonzero coefficients. Thus, the commutation error is determined by the filter moments, $M^k(\xi)$, and mapping function, $F(\xi)$.

In this report we consider a general class of filters which satisfy the following properties:

$$M^0(\xi) = 1 \text{ for } \xi \in [\alpha, \beta]; \tag{8a}$$

$$M^k(\xi) = 0 \text{ for } k = 1, \ldots, n-1 \text{ and } \xi \in [\alpha, \beta]; \tag{8b}$$

$$M^k(\xi) \text{ exist for } k \geq n. \tag{8c}$$

There are many examples of filters which satisfy these properties when the function $\phi(\xi)$ is defined in the domain $(-\infty, +\infty)$. One is the exponentially decaying filter defined in (Van der Ven, 1995). Another example is the correlation function of the Daubechies scaling function used in multi-resolution analysis for constructing orthonormal wavelet bases (Beylkin, 1995; Beylkin and Saito, 1993). Examples of such filters with 5, 9, and 17 vanishing moments and the corresponding Fourier transforms, $\hat{G}(k) = \int_{-\infty}^{+\infty} G(\xi)\exp(-ik\xi)d\xi$, are shown in Fig. 1.

We also note that the definition (8) does not require that the filter kernel be symmetric. This allows us to use a wider class of filters than in (Ghosal and Moin, 1995; Van der Ven, 1995). We do not present continuous filters on an interval, which satisfy definitions (8a-8c), since as it will be shown later, for practical purposes we need discrete filters. For now we only assume that such filters exist and that they can be constructed.

Using properties (8a) and (8b) it follows that

$$\frac{\partial M^k}{\partial \xi}(\xi) = 0 \quad \text{for} \quad k = 0, \ldots, n-1. \tag{9}$$

Consequently, the commutation error (7) is

$$\left[\frac{d\psi}{dx}\right] = \mathrm{O}(\Delta^n). \tag{10}$$

It is easy to show that in the homogeneous (periodic) case, when the shape of the filter does not depend on the location, and the mapping from the physical to the computational domain is linear, A_k is exactly zero for any k and the filter moments are not functions of the location. This results in zero commutation error.

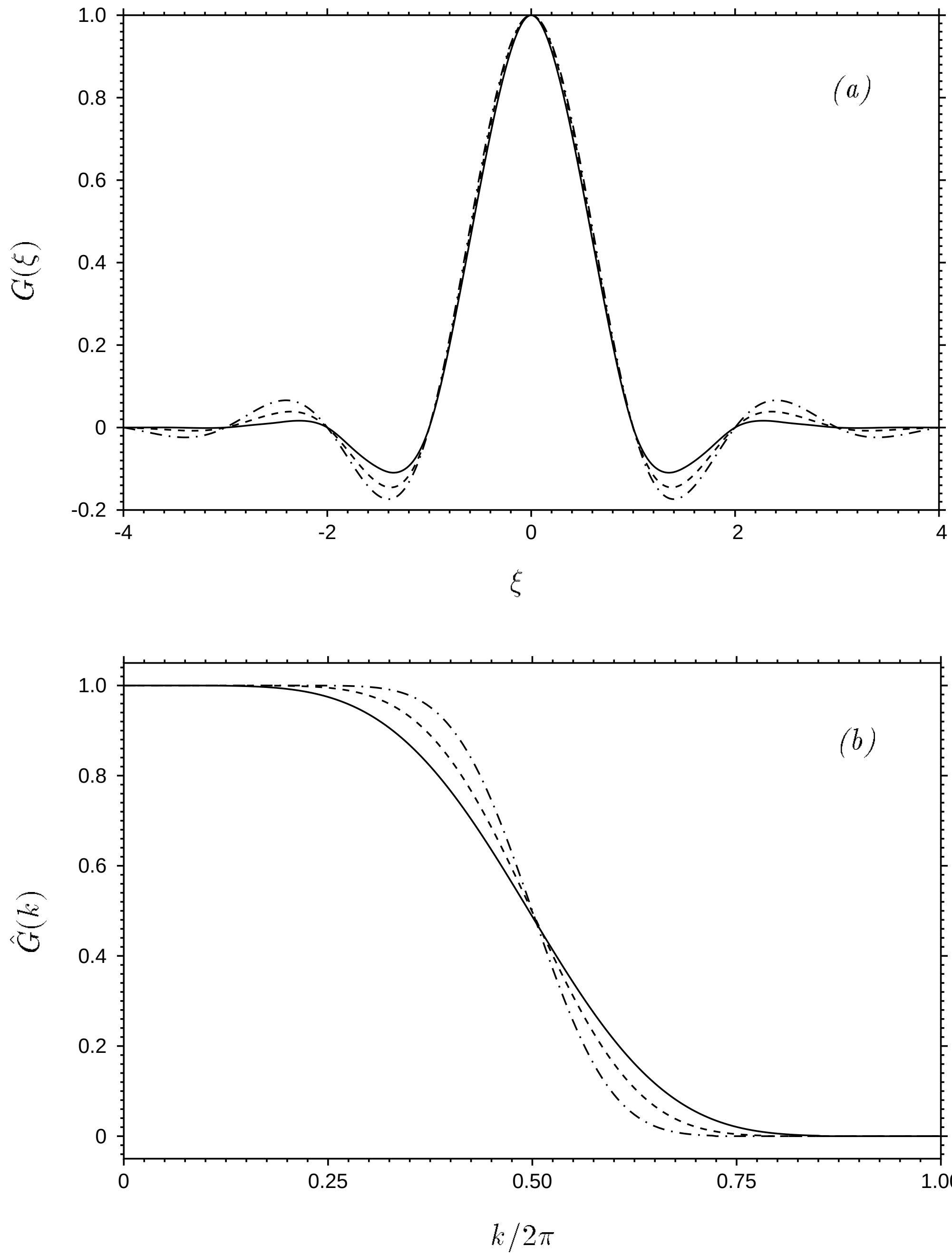

FIGURE 1. Filters $G(\xi)$, (a), with 5 (——), 9 (- - - -), and 17 (—·—) vanishing moments and corresponding Fourier transforms $\hat{G}(k)$, (b).

The non-uniform filtering operation in one spatial dimension can be extended easily to three spatial dimensions (see VLM). As in the one-dimensional case this transformation can be associated with the mapping of spatially non-uniform computational grid to a uniform grid with spacings $\Delta_1,\ \Delta_2,\ \Delta_3$ in the corresponding directions. If one performs the same type of analysis as in one-dimensional case, it is easy to show (see VLM) that the commutation error in three spatial dimensions is given by

$$\left[\frac{\partial \psi}{\partial x_k}\right] = \mathrm{O}(\Delta_1^n, \Delta_2^n, \Delta_3^n). \tag{11}$$

Thus, the commutation error of differentiation and filtering operation is no more than the error introduced by an n-th order finite difference scheme, provided that the filter has $n-1$ zero moments.

2.2 Discrete filtering in complex geometry

In large eddy simulation of turbulent flows, the solution is available only on a set of discrete grid points, and thus discrete filters are required in various operations. The machinery developed in Section 2.1 can be adapted to discrete filtering. In this section we will limit ourselves to consideration of discrete one-dimensional filtering, since three dimensional filtering can be considered as an application of a sequence of three one-dimensional filters. Also, since the filtering operation is performed in the mapped space, we will consider only the case of uniformly sampled data.

2.2.1 Construction of discrete filters

Let us consider a one-dimensional field $\phi(\xi)$ defined in the domain $[\alpha, \beta]$. $\{\phi_j\}$ corresponds to values of $\phi(\xi_j)$ at locations $\xi_j = \alpha + \Delta j$ $(j = 0, \ldots, N)$, where Δ is the sampling interval. A one-dimensional filter is defined by

$$\frac{1}{\Delta} G\left(\frac{\xi_j - \eta}{\Delta}, \xi_j\right) = \sum_{l=-K_j}^{L_j} \mathrm{w}_l^j \delta(\eta - \xi_{j+l}), \tag{12}$$

where $\delta(\xi)$ is the Dirac δ-function and w_l^j are weight factors. We consider the general class of non-symmetric filters for which $K_j \neq L_j$. One of the important aspects of discrete filters is that all filter moments exist and the radii of convergence of Taylor series (5) and other related series are infinite. Substitution of (12) into (1) gives the following definition for a discrete filter

$$\overline{\phi}_j = \sum_{l=-K_j}^{L_j} \mathrm{w}_l^j \phi_{j+l}. \tag{13}$$

It is the property (12) which allows us to apply results of Section 2.1 to discrete filters.

In light of the filter definition (8), the weight factors should satisfy the following properties

$$\sum_{l=-K_j}^{L_j} \mathrm{w}_l^j = 1, \tag{14a}$$

$$\sum_{l=-K_j}^{L_j} l^m \mathrm{w}_l^j = 0, \quad m = 1, \ldots n-1. \tag{14b}$$

Equations (14) give us n constraints on w_l^j and are solvable if and only if $L_j + K_j + 1 \geq n$. If $L_j + K_j + 1 > n$ then additional constraints can be applied.

Conditions (14) give the minimum number of degrees of freedoms for a discrete filter in order for the derivative and filtering operations to commute to order n. This condition gives the minimum filter support, which can be increased by adding additional constraints. The additional linear or nonlinear constraints can be altered depending on the desired shape of the Fourier transform $\hat{G}(k)$ associated with the filter (12) given by

$$\hat{G}(k) = \sum_{l=-K_j}^{L_j} \mathrm{w}_l^j e^{-i\Delta k l}. \tag{15}$$

case	number of vanishing moments	w_{-3}	w_{-2}	w_{-1}	w_0	w_1	w_2	w_3	w_4	w_5
1	1			$\frac{1}{4}$	$\frac{1}{2}$	$\frac{1}{4}$				
2	2				$\frac{7}{8}$	$\frac{3}{8}$	$-\frac{3}{8}$	$\frac{1}{8}$		
3	2			$\frac{1}{8}$	$\frac{5}{8}$	$\frac{3}{8}$	$-\frac{1}{8}$			
4	3				$\frac{15}{16}$	$\frac{1}{4}$	$-\frac{3}{8}$	$\frac{1}{4}$	$-\frac{1}{16}$	
5	3			$\frac{1}{16}$	$\frac{3}{4}$	$\frac{3}{8}$	$-\frac{1}{4}$	$\frac{1}{16}$		
6	3		$-\frac{1}{16}$	$\frac{1}{4}$	$\frac{5}{8}$	$\frac{1}{4}$	$-\frac{1}{16}$			
7	4				$\frac{31}{32}$	$\frac{5}{32}$	$-\frac{5}{16}$	$\frac{5}{16}$	$-\frac{5}{32}$	$\frac{1}{32}$
8	4			$\frac{1}{32}$	$\frac{27}{32}$	$\frac{5}{16}$	$-\frac{5}{16}$	$\frac{5}{32}$	$-\frac{1}{32}$	
9	4		$-\frac{1}{32}$	$\frac{5}{32}$	$\frac{11}{16}$	$\frac{5}{16}$	$-\frac{5}{32}$	$\frac{1}{32}$		
10	5	$\frac{1}{64}$	$-\frac{3}{32}$	$\frac{15}{64}$	$\frac{11}{16}$	$\frac{15}{64}$	$-\frac{3}{32}$	$\frac{1}{64}$		

TABLE 1. The values of the weight factors and the number of vanishing moments for different minimally constrained discrete filters.

A desirable constraint on a filter is that its Fourier transform be zero at the cut-off frequency, *i.e.* $\hat{G}(\pi/\Delta) = 0$. The mathematical equivalent of this requirement is given by

$$\sum_{l=-K_j}^{L_j} (-1)^l \mathrm{w}_l^j = 0. \tag{16}$$

Condition (14) and (16) represent the minimum number of constraints which should be imposed on the filter. Examples of weights for minimally constrained discrete filters are given in Table 1 and associated Fourier transforms for some of these filters are presented in Figs. 2-4. Examples of the Fourier transforms of minimally constrained symmetric filters with one, three, and five vanishing moments are presented

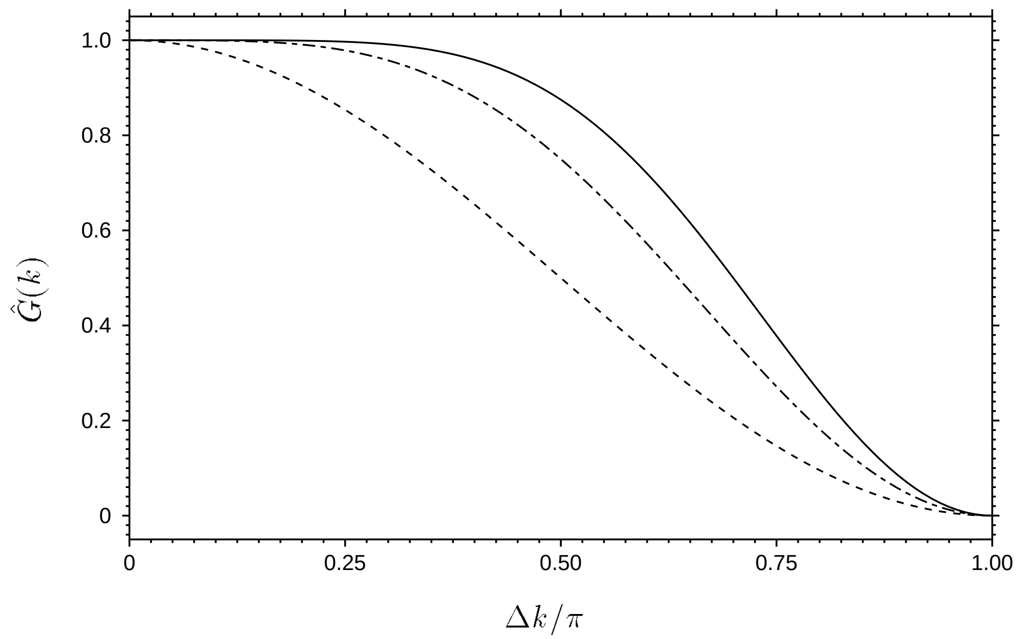

FIGURE 2. Fourier transform $\hat{G}(k)$ of the symmetric minimally constrained discrete filters with one (- - - -), three (— · —), and five (———) vanishing moments corresponding respectively to cases 1, 6, and 10 given in Table I.

in Fig. 2. These filters correspond respectively to cases 1, 6, and 10 presented in Table 1. We see that increasing the number of vanishing moments yields a better approximation to the sharp cutoff filter, which is more appealing from a physical point of view. It also can be observed that filters shown in Fig. 2 have different effective cut-off frequencies. Thus, in order to control the effective cut-off frequency, additional constraints should be introduced. The Fourier transform of asymmetric filters with four vanishing moments corresponding to cases 8 and 9 presented in Table 1 are shown in Figs. 3 and 4 correspondingly. Note that the asymmetric filters introduce phase shifts due to their non-zero imaginary parts. The imaginary part should be minimized by introducing additional constraints. Also notice the overshoot in the real part and absolute value of the filter shown in Fig. 3. In general, an overshoot is not desirable since it may lead to non-physical growth of energy. Additional constraints are necessary in order to reduce or remove overshoot.

In the interior of the domain, in order to eliminate the phase shift, the filter should be symmetric, *i.e.* the following relation should be satisfied

$$\mathrm{w}_l^j = \mathrm{w}_{-l}^j, \quad l = 1, \ldots, L, \tag{17a}$$

$$L_j = K_j = L. \tag{17b}$$

In this case the filter only adjusts the amplitude of a given wavenumber component of the solution and leaves its phase unchanged. Near the boundaries, however,

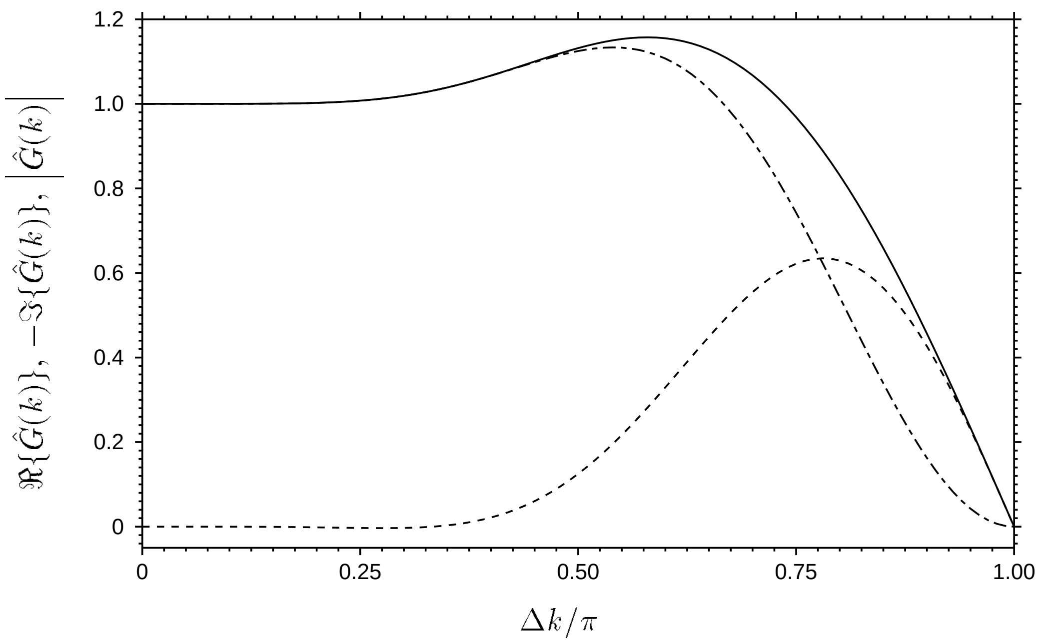

FIGURE 3. Real $\Re\{\hat{G}(k)\}$ (—·—), imaginary $\Im\{\hat{G}(k)\}$ (- - - -), and absolute value $\left|\hat{G}(k)\right|$ (———) of Fourier transform $\hat{G}(k)$ of the asymmetric discrete filter with four vanishing moments corresponding to case 8 given in Table I.

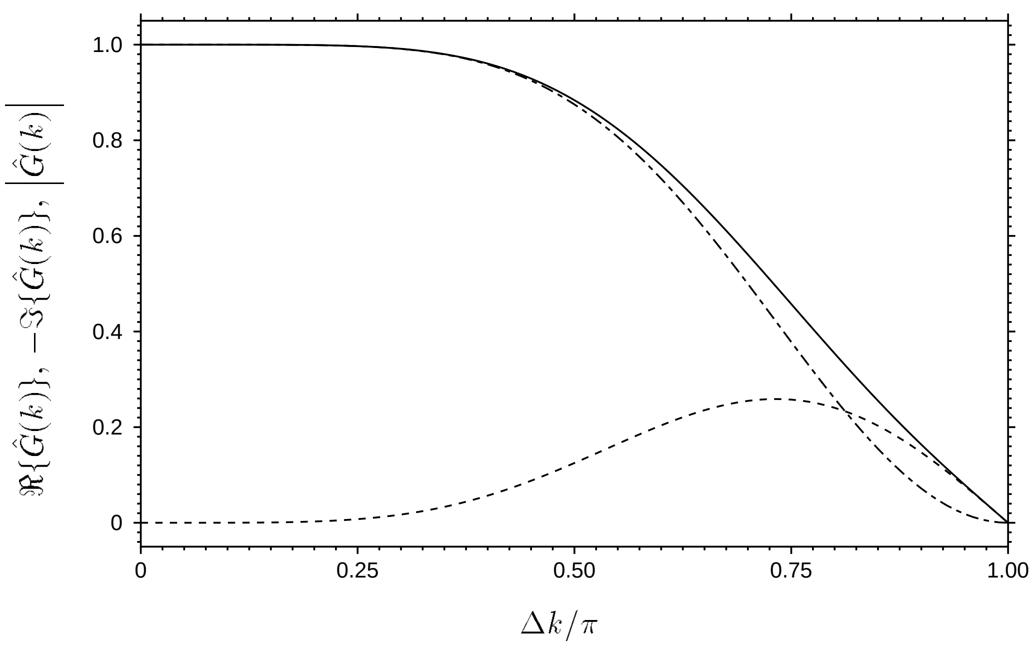

FIGURE 4. Real $\Re\{\hat{G}(k)\}$ (—·—), imaginary $\Im\{\hat{G}(k)\}$ (- - - -), and absolute value $\left|\hat{G}(k)\right|$ (———) of Fourier transform $\hat{G}(k)$ of the asymmetric discrete filter with four vanishing moments corresponding to case 9 given in Table I.

case	number of vanishing moments	additional constraints	w_0	$w_{\pm1}$	$w_{\pm2}$	$w_{\pm3}$	$w_{\pm4}$	$w_{\pm5}$
1	3	$\hat{G}(\Delta\pi/3) = 1/2$ $\hat{G}^{(m)}(\Delta\pi) = 0, m = 0, \ldots, 5$	$\frac{373}{1152}$	$\frac{911}{3456}$	$\frac{203}{1728}$	$-\frac{11}{2304}$	$-\frac{203}{6912}$	$-\frac{61}{6912}$
2	3	$\hat{G}(\Delta\pi/2) = 1/2$ $\hat{G}^{(m)}(\Delta\pi) = 0, m = 0, \ldots, 1$	$\frac{1}{2}$	$\frac{9}{32}$	0	$-\frac{1}{32}$		
3	3	$\hat{G}(2\Delta\pi/3) = 1/2$ $\hat{G}^{(m)}(\Delta\pi) = 0, m = 0, \ldots, 1$	$\frac{47}{72}$	$\frac{35}{144}$	$-\frac{11}{144}$	$\frac{1}{144}$		

TABLE 2. The values of the weight factors and the number of vanishing moments for different linearly constrained discrete filters.

it may be necessary to make the filter asymmetric. In this case a phase shift is introduced and one is interested in minimizing this effect.

Examples shown in Figs. 2-4 demonstrate the necessity of the introduction of additional constraints which ensure that the resulting filter has all the desired properties. One way to constrain the filter is to specify either its value or the value of its derivative for a given frequency k_s. Examples of weights for filters with three vanishing moments and different linear constraints are given in Table 2 and associated Fourier transforms for these filters are presented in Fig. 5. These filters are constrained in such a way that the effective filter widths are 3Δ, 2Δ, and $3/2\Delta$ (corresponding to characteristic wavenumbers $\Delta k_s/\pi = 1/3, 1/2, 2/3$). We observed that for the filters with relatively small characteristic wavenumbers, the number of zero derivatives at $k = \pi/\Delta$ should be considerably larger than for filters with characteristic wavenumbers close to π/Δ. If we chose this number small enough, then the value of the Fourier transform of the filter for frequencies larger then characteristic wavenumber may reach a large amplitude. Thus setting the large number of derivatives at $k = \pi/\Delta$ forces the filter to have the desired shape.

2.2.2 Alternative construction of filters with desired properties

Linear constraints are often enough to obtain the desired filter. However, there are situations, especially for non-symmetric filters, where it is difficult to choose a limited number of constraints such that the filter is close to the desired shape. It is much more desirable to specify the target filter function $\hat{G}_t(k)$ and to construct a filter which will be close to it. One way of doing so is to find the set of filter weights which satisfy all linear constraints and minimize a following functional

$$\int_0^{\pi/\Delta} \left(\Re\left\{\hat{G}(k) - \hat{G}_t(k)\right\}\right)^2 dk + \int_0^{\pi/\Delta} \left(\Im\left\{\hat{G}(k) - \hat{G}_t(k)\right\}\right)^2 dk, \qquad (18)$$

where $\Re\{z\}$ and $\Im\{z\}$ denote correspondingly real and imaginary parts of a complex number z. Note that integral ranges as well as relative weights for real and imaginary contributions to the functional can be arbitrarily set depending on the

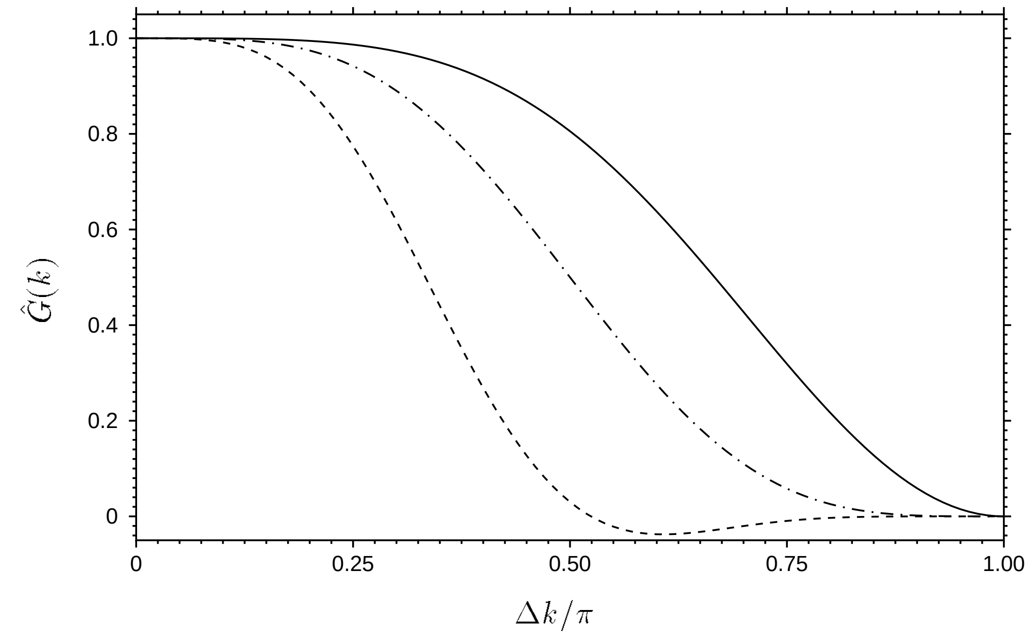

FIGURE 5. Fourier transform $\hat{G}(k)$ of the symmetric discrete filters with different additional linear constraints corresponding to cases 1 (- - - -), 2 (— · —), and 3 (———) given in Table II.

filter function $\hat{G}_t(k)$. The mathematical details of the minimization are given in VLM. Figure 6(a) shows an example of an asymmetric filter with eight point stencil, ($K = 2$ and $L = 5$). The real part of the filter is constrained to be 1/2 at $\Delta k/\pi = 1/2$. The filter value and its first two derivatives are constrained to be zero at $k = \pi/\Delta$. In order to improve the filter's characteristics, the minimization was performed, where requirements for two derivatives at $k = \pi/\Delta$ were relaxed and quadratic minimization as described in VLM was used instead. The resulting filter is shown in Fig. 6(b). Comparing both filters we can see that the filter presented in Fig. 6(b) has better characteristics. We found that, in general, minimization procedure gives better filters than the ones obtained using only linear constraints.

2.2.3 Pade filters

Discrete filters with vanishing moments are not limited to the simple weighted average form of (13). Pade-type filters are described in this subsection as an example of an alternative formulation. Other discrete filtering approaches can be utilized as well but they will not be discussed here. A Pade filter is defined as

$$\sum_{m=-M_j}^{N_j} \mathrm{v}_m^j \overline{\phi}_{j+m} = \sum_{l=-K_j}^{L_j} \mathrm{w}_l^j \phi_{j+l}, \tag{19}$$

and requires the solution of linear systems of equations. The Fourier transform

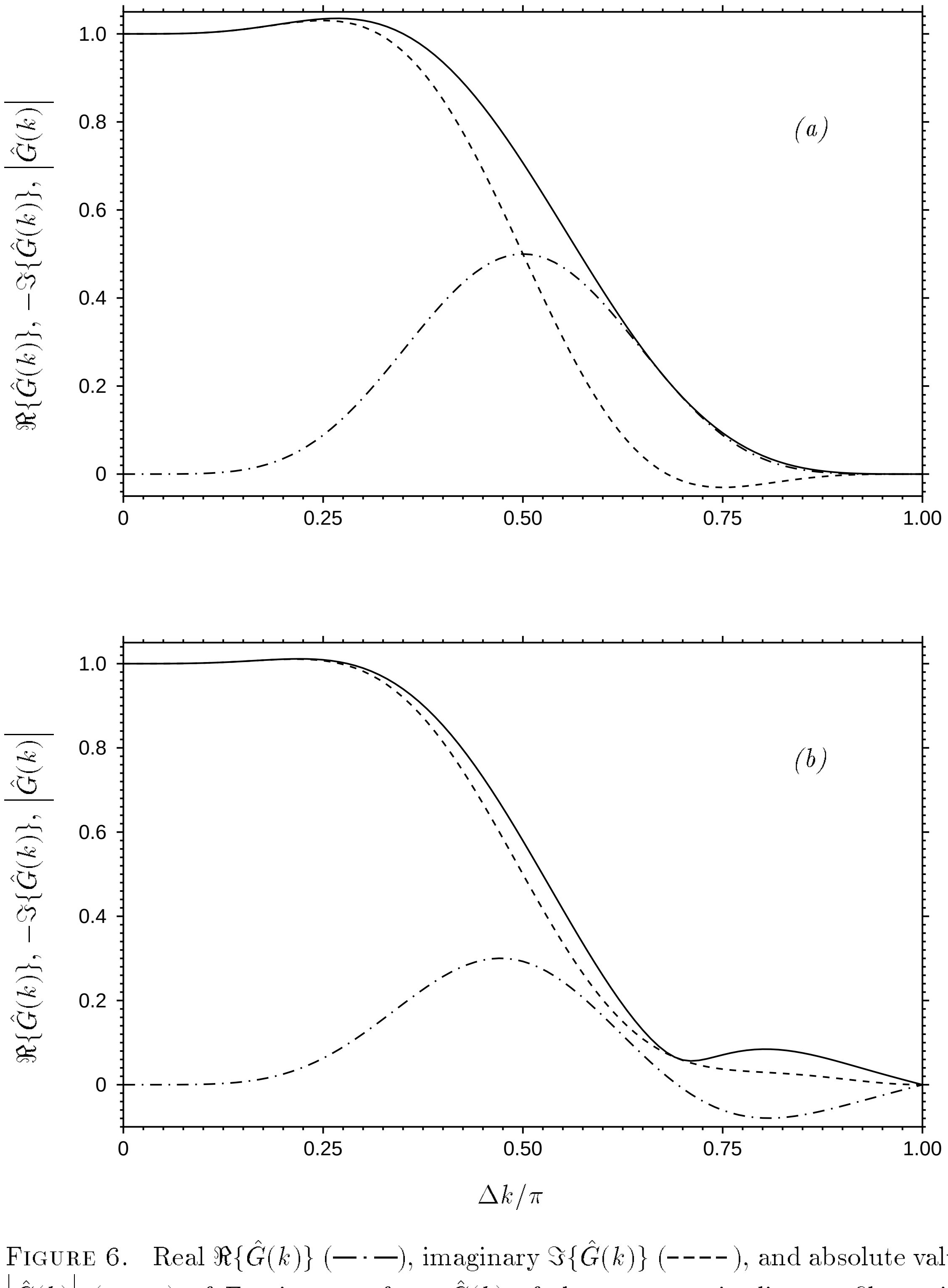

FIGURE 6. Real $\Re\{\hat{G}(k)\}$ (—·—), imaginary $\Im\{\hat{G}(k)\}$ (- - - -), and absolute value $\left|\hat{G}(k)\right|$ (———) of Fourier transform $\hat{G}(k)$ of the asymmetric discrete filter with three vanishing moments obtained using only linear constraints (a) and quadratic minimization (b).

case	additional constraints	v_0	$v_{\pm1}$	$v_{\pm2}$	$v_{\pm3}$	w_0	$w_{\pm1}$	$w_{\pm2}$	$w_{\pm3}$	$w_{\pm4}$	$w_{\pm5}$
1	$\hat{G}(\Delta\pi/3) = 1/2$ $\hat{G}^{(m)}(\Delta\pi) = 0,\ m = 0, \dots, 9$	$\frac{543}{128}$	$-\frac{1405}{512}$	$\frac{313}{256}$	$-\frac{51}{512}$	$\frac{63}{256}$	$\frac{105}{512}$	$\frac{15}{128}$	$\frac{45}{1024}$	$\frac{5}{512}$	$\frac{1}{1024}$
2	$\hat{G}(\Delta\pi/2) = 1/2$ $\hat{G}^{(m)}(\Delta\pi) = 0,\ m = 0, \dots, 7$	$\frac{7}{12}$	0	$\frac{5}{24}$		$\frac{7}{24}$	$\frac{175}{768}$	$\frac{5}{48}$	$\frac{35}{1536}$	0	$-\frac{1}{1536}$
3	$\hat{G}(2\Delta\pi/3) = 1/2$ $\hat{G}^{(m)}(\Delta\pi) = 0,\ m = 0, \dots, 3$	$\frac{49}{120}$	$\frac{13}{60}$	$\frac{19}{240}$		$\frac{11}{30}$	$\frac{119}{480}$	$\frac{1}{15}$	$\frac{1}{480}$		

TABLE 3. The values of the weight factors for different linearly constrained symmetric Pade filters with five vanishing moments.

$\hat{G}(k)$ associated with Pade-type filters is given by

$$\hat{G}(k) = \frac{\sum_{l=-K_j}^{L_j} w_l^j e^{-i\Delta kl}}{\sum_{m=-M_j}^{N_j} v_m^j e^{-i\Delta km}}. \tag{20}$$

In the case of Pade filters conditions (14) can be rewritten as

$$\sum_{l=-K_j}^{L_j} w_l^j = 1, \tag{21a}$$

$$\sum_{m=-M_j}^{N_j} v_m^j = 1, \tag{21b}$$

$$\sum_{m=-M_j}^{N_j} m^i v_m^j = \sum_{l=-K_j}^{L_j} l^i w_l^j, \quad i = 1, \dots n-1. \tag{21c}$$

It is straightforward to constrain Pade filters to a specific value at specific frequency. Nevertheless linear constraining of filter derivatives $\hat{G}^{(m)}(k)$ at certain frequency requires additional specification of filter value as well as all previous derivatives. For more details on Pade filters we refer to (Lele, 1992).

The use of Pade-type filters gives more flexibility in constructing filters which are closer to spectral cut-off filters. Examples of weights for symmetric ($M_j = N_j$ and $K_j = L_j$) Pade filters with five vanishing moments and different linear constraints are given in Table 3 and associated Fourier transforms are presented in Fig. 7. Comparing Figs. 5 and 7 it can be seen that Pade filters are considerably better approximations of sharp cut-off filters.

2.2.4 Commutation error of discrete filtering and differentiation

In Section 2.1 we demonstrated that the commutation error of continuous filtering and differentiation operators is determined by the number of vanishing moments

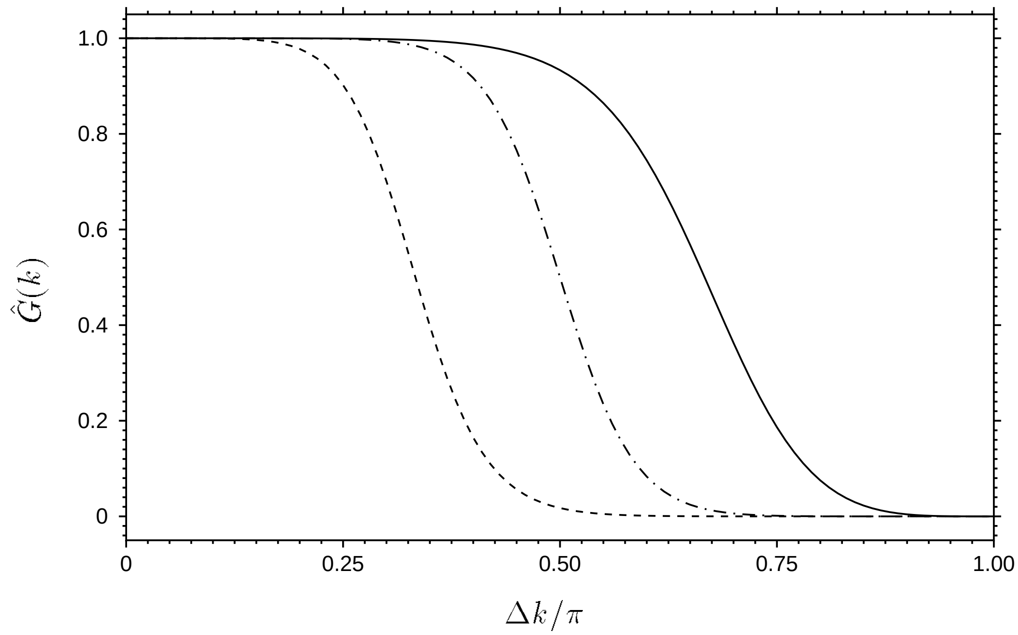

FIGURE 7. Fourier transform $\hat{G}(k)$ of the symmetric Pade filters with different additional linear constraints corresponding to cases 1 (- - - -), 2 (— · —), and 3 (———) given in Table III.

of the continuous filter. As it was mentioned earlier in this section the same conclusion is valid for discrete filters. In order to validate that discrete filtering and differentiation commute up to the same order, we perform a numerical test in which we differentiate numerically the Chebyshev polynomial of the 16-th order and determine the commutation error of discrete filtering and differentiation operators. Since the derivative of the Chebyshev polynomial can be calculated exactly, we can calculate the truncation error of the numerical differentiation as well. We choose the nonuniform computational mesh to be given by

$$x_j = -\frac{\tanh\left(\gamma\left(1-\frac{2j}{N_g}\right)\right)}{\tanh(\gamma)}, \tag{22}$$

where N_g is the total number of grid points and γ is the stretching parameter. The choice for the hyperbolic grid stretching is motivated by its frequent use in both DNS and LES simulations of wall-bounded flows. For the hyperbolic tangent grid the ratio of largest to smallest grid size is a function of stretching parameter γ and is given by $\cosh^3\gamma/\sinh\gamma$. In this test we choose $\gamma = 2.75$, which makes this ratio approximately 62. The differentiation operator is chosen to be fourth order accurate on the non-uniform grid. Figure 8 shows the truncation error of finite difference scheme and commutation errors as a function of the total number of grid points for filters with different number of zero moments. The results presented on Fig. 8 confirm that the discrete filtering and differentiation operators commute up to the n-th order, provided that discrete filter has $n-1$ vanishing moments.

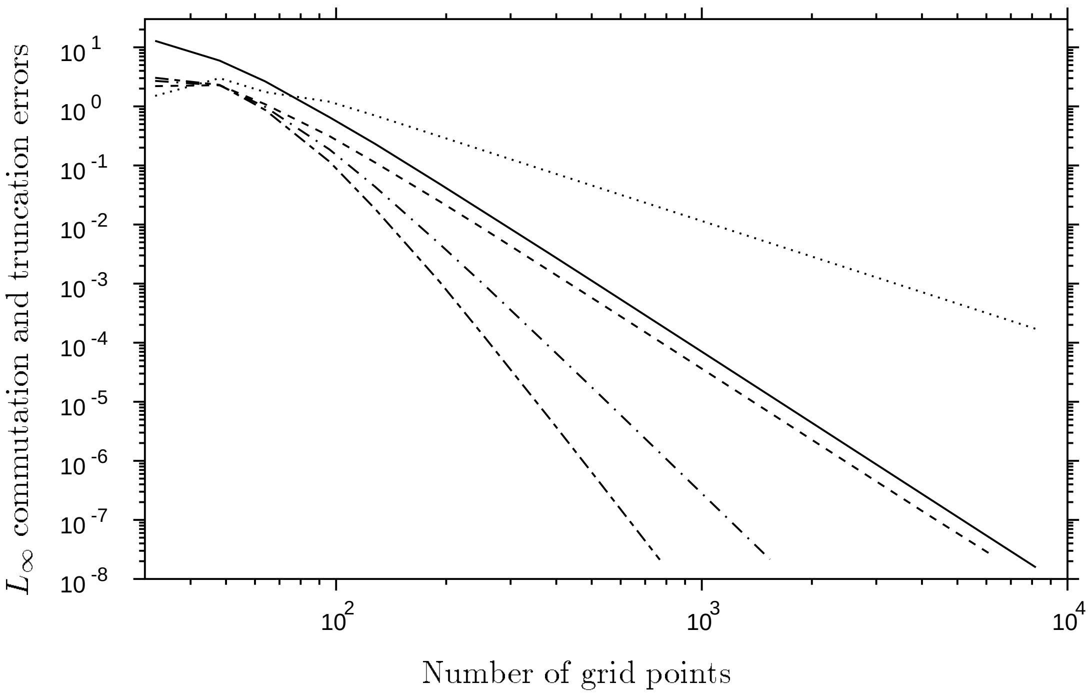

FIGURE 8. Truncation error (——) of the differentiation operator and commutation error for discrete filtering and differentiation operations for the filters with one (········), three (– – – –), five (— · —), and seven (— – —) vanishing moments.

2.3 Conclusions

We have formulated general requirements for a filter having a non-uniform filter width which ensure that the differentiation and filtering operations commute to any desired order. Minimization of the commutation error is achieved by requiring that the filter has a number of vanishing moments. Application of this filter to the Navier-Stokes equations results in the standard LES equations which can be solved on a non-uniform computational grid. The commutation error can be neglected provided that the filter has $n-1$ vanishing moments, where n is the order of the numerical discretization scheme used to solve the LES equations. A general set of rules for constructing discrete filters in complex geometries is provided. The use of these filters ensures consistent derivation of discrete LES equations. The resulting discrete filtering operation is very simple and efficient.

3. Future plans

The commutative discrete filters presented in this report enable us to perform consistent large eddy simulations of inhomogeneous turbulent flows. The first step in this direction is to study the effect of explicit filtering in LES of turbulent channel flow. For that purpose we are planning to use the fourth-order scheme described in (Morinishi *et al.*, 1997). A discrete filter with a number of vanishing moments will be applied to the incremental field at the conclusion of each time step. This procedure guarantees that no high frequency signal is added to the field from the previous time step. The dynamic procedure should be modified due to explicit filtering of nonlinear terms. As more experience is gained with the explicit filtering, it will be determined whether explicit filtering is a cost-effective means of improving simulation results. If so, explicit filtering will be applied to more complicated problems.

REFERENCES

BEYLKIN, G. 1992 On the representation of operators in bases of compactly supported wavelets. *SIAM J. Numer. Anal.* **29,** 1716-1740.

BEYLKIN, G. & SAITO, N. 1993 Wavelets, their autocorrelation functions, and multiresolution representation of signals. In *Proceedings of SPIE*, **LB26**, 39-50.

GERMANO, M., PIOMELLI, U., MOIN, P. & CABOT, W. H. 1991 A dynamic subgrid-scale eddy viscosity model. *Phys. Fluids A.* **3,** 1760-1765.

GHOSAL, S., LUND, T. S., MOIN, P., & AKSELVOLL, K. 1995 A dynamic localization model for large-eddy simulation of turbulent flows. *J. Fluid Mech.* **286,** 229-255.

GHOSAL S. & MOIN P. 1995 The basic equations of the large eddy simulation of turbulent flows in complex geometry. *J. Comp. Phys.* **118,** 24-37.

LELE, S. K. 1992 Compact finite difference schemes with spectral-like resolution. *J. Comp. Phys.* **103,** 16-42.

LEONARD, A. 1974 Energy cascade in large-eddy simulations of turbulent fluid flows. *Adv. Geophys.* **18,** 237-248.

LUND, T. S. & KALTENBACH, H.-J. 1995 Experiments with explicit filtering for LES using a finite-difference method. In *Annual Research Briefs*, Center for Turbulence Research, NASA Ames/Stanford Univ., 91-105.

MORINISHI, Y., LUND, T. S., VASILYEV, O. V., & MOIN, P 1997 Fully Conservative Higher Order Finite Difference Schemes for Incompressible Flow. *Submitted to J. Comp. Phys.*

VAN DER VEN, H. 1995 A family of large eddy simulation (LES) filters with nonuniform filter widths. *Phys. Fluids.* **7,** 1171-1172.

VASILYEV, O. V., LUND, T. S., & MOIN, P. 1997 A General Class of Commutative Filters for LES in Complex Geometries. *Submitted to J. Comp. Phys.*